Induced phase shift in interlayer magnetic exchange coupling: Magnetic layer doping

U. Ebels, R. L. Stamps,* L. Zhou, and P. E. Wigen
Department of Physics, Ohio State University, Columbus, Ohio 43210

K. Ounadjela
IPCMS, CNRS, UMR46, 23 rue du Loess, F-67037 Strasbourg, France

J. Gregg
Clarendon Laboratory, University of Oxford, Oxford OX1 3PU, United Kingdom

J. Morkowski and A. Szajek
Institute of Molecular Physics, Polish Academy of Sciences, Smoluchowskiego 17, 16-179 Poznan, Poland
(Received 22 December 1997; revised manuscript received 27 March 1998)

The changes in the phase of the long-period oscillatory interlayer exchange coupling between two Co layers, separated by a Ru spacer layer, are examined as a function of small concentrations of Ag, Au, Cu, and Ru added to the magnetic Co layer. Phase changes of up to 360° are observed for small concentrations of Ag (up to 8%) with minimal modifications to the coupling period or strength. In addition, an additive antiferromagnetic bias is observed for small interlayer thicknesses, indicative of a superexchange contribution to the interlayer coupling. The effects are also investigated for Cu as the nonmagnetic spacer material and phase shifts are observed similar to those in the systems with Ru as the spacer material. Band-structure calculations are presented that show that insertion of small amounts of Ag into the Co host leads to additional states at the bottom of the band. This lowering of the lower band limit is interpreted as a change in the potential step that determines the spin-dependent reflection coefficients of the electrons crossing the ferromagnet/spacer layer interface. The observed phase shifts are therefore interpreted to directly result from changes in the band structure of the ferromagnetic layer. The insertion of small amounts of nonmagnetic material in the ferromagnetic layer thus provides a mechanism with which the phase of the coupling can be shifted in a well controllable manner. [S0163-1829(98)06433-9]

I. INTRODUCTION

The oscillatory interlayer exchange coupling between two ferromagnetic layers separated by a nonmagnetic spacer layer has received considerable attention in the past years.[1–4] The mechanism responsible for this indirect oscillatory exchange coupling is by now widely accepted to result from the confinement of the electrons in the spacer-layer material[5–11] due to the multiple reflections of the electron waves at the interfaces and surfaces. Within this quantum interference description the coupling *period* is largely determined by the topology of the Fermi surface of the nonmagnetic spacer layer, whereas the coupling *strength* and the coupling *phase*[12] are also strongly influenced by the magnetic-layer and cap-layer properties. In particular, it was predicted[11,13] and confirmed experimentally[14–16] that the coupling strength oscillates as a function of the magnetic-layer and cap-layer thickness. Furthermore, experiments show that the coupling phase of the short-period oscillation can be shifted as a function of the magnetic-layer composition upon going from pure Co layers via a $Co_{50}Ni_{50}$ alloy to pure Ni layers.[17,18] This result can be understood qualitatively from the fact that the phase of the coupling as a function of the interlayer thickness is directly related to the phase of the spin-dependent complex reflection coefficients at the interfaces.[11,17] More specifically, since the reflection coefficients are determined by the details of the electronic properties of the nonmagnetic spacer layer as well as of the magnetic layer, changes in the electronic structure of the magnetic layer will be reflected in a change of the coupling phase. This is evident from the experiment[17,18] and theoretical[19] investigations of the dependence of the coupling phase on the number of electrons in the magnetic layer by varying the concentration in Co_xFe_{1-x} and Co_xNi_{1-x} alloys from $x=1$ to $x=0$.

In contrast to these large compositional changes, here experiments are described for trilayer systems in which the composition of the magnetic layer is only slightly modified by adding small amounts of a nonmagnetic material to the magnetic layer.[20] It is shown that by increasing the concentration of the nonmagnetic material from zero to a few percent, the coupling phase can be shifted in a continuous manner from 0° to 360°. Band-structure calculations are presented that show that for the small concentrations used, the electronic band structure at the Fermi surface is only slightly perturbed. The major modifications are additional states at the bottom of the band, which are interpreted as an increase of the potential step for the electrons crossing the interface. Using a two-band tight-binding model it is shown that this potential step may result in a significant phase shift in the oscillatory interlayer coupling.

Besides the observed shift in the coupling phase, the addition of nonmagnetic materials to the magnetic layer also reveals an additive antiferromagnetic bias for small inter-

layer thicknesses that is independent of the doping concentration and that is indicative of a superexchange bias as described by Shi, Levy, and Fry.[21]

For the studies of the phase shift, a total of 120 trilayers were grown consisting of either pure Co layers or Co layers with small amounts of Ag, Au, Cu, or Ru added. In the following, the addition of small amounts of nonmagnetic materials into the Co layer is called ''doping,'' as in a broader sense it modifies its electronic properties, as will be seen in Sec. V. In the case of Cu, Au, and Ru, a substitutional alloy forms with the Co host and in the case of Ag an immiscible solid solution forms. Clustering was discouraged by holding the substrate at low temperatures (240 K) during growth and by introducing only small concentrations ($\leqslant 8\%$), which furthermore guarantees that the magnetic properties are not modified. For the spacer material, either Ru or Cu was chosen. The spacer-layer constitution itself was left unaltered in order not to perturb the interlayer band structure and the magnetic-layer and cap-layer thicknesses were held constant for varying doping concentrations.

The paper is organized as follows. The preparation and structure of the trilayer systems are discussed in Sec. II. In Sec. III the magnetization and ferromagnetic resonance experiments are described from which the amplitude, period, and phase of the oscillatory exchange coupling are deduced. The results obtained for the Co/Ru/CoAg and CoAg/Cu/CoAg structures are presented in Sec. IV. In Sec. V a mechanism for the Ag-caused phase shift is presented, supported by band-structure calculations on Ag-doped Co. Additional experiments on Co/Ru/CoM trilayers with $M=$ Au, Cu, and Ru dopants are discussed in Sec. VI together with further results on interface effects in the Co/Cu structures. In Sec. VII the possibility of an additional superexchange bias at small interlayer thicknesses is indicated.

II. SAMPLE PREPARATION AND STRUCTURE

The samples were prepared in UHV by *e*-beam epitaxy on a smooth, clean 100-Å-thick single crystalline hcp (0001) Ru buffer layer. The buffer layer was deposited on a mica substrate at a pressure less than 2×10^{-10} mbar. The reflection high-energy electron-diffraction (RHEED) patterns obtained during the sample growth reveal well-defined structures. This suggests the realization of good crystalline quality throughout the deposition. An example RHEED pattern is shown in Fig. 1 for a Co trilayer doped with Ag. The quality of the Ru buffer layer is evident from the narrowness of the streaks and the presence of a 2×2 reconstruction.

For the systems with Ru as the spacer-layer material, a pure 32-Å Co layer was grown on a Ru buffer layer and then followed with a Ru layer. The Ru spacer layer was then sandwiched under a doped Co layer. RHEED patterns during growth are shown in Fig. 1 along with two different azimuths. Figures 1(a) and 1(b) are patterns taken after deposition of the Ru buffer layer. Figures 1(c) and 1(d) show patterns after deposition of the pure Co layer. It can be seen from these patterns that the pure Co grows epitaxially on the Ru buffer layer with the hexagonal basal plane parallel to the surface. A significant fcc (111) character was found for the growth of the pure Co layer, with a high concentration of stacking faults indicating a mixture of fcc and hcp. After

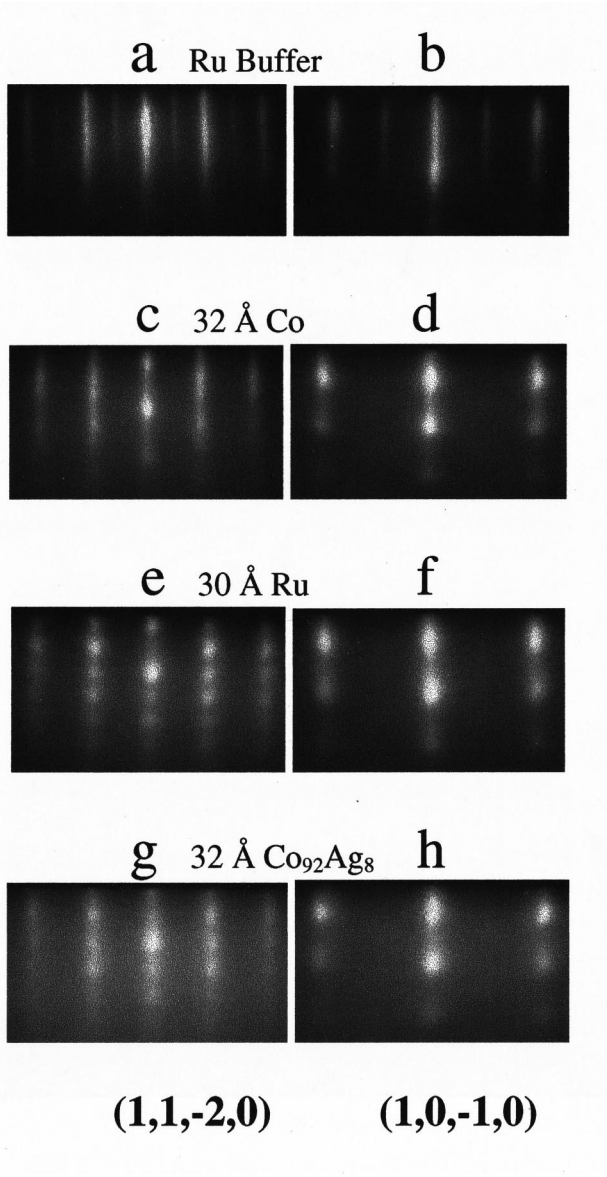

FIG. 1. RHEED patterns observed during growth along two azimuths for the Ru buffer layer and subsequent growth of the Co/Ru/$Co_{92}Ag_8$ layers. Patterns are shown after deposition of the 100-Å-thick Ru layer in (a) and (b), after deposition of the first pure 32-Å Co layer in (c) and (d), after deposition of a 30-Å-thick Ru spacer layer in (e) and (f), and after deposition of a 32-Å-thick $Co_{92}Ag_8$ layer.

deposition of a 30-Å Ru spacer layer, shown in Figs. 1(e) and 1(f), the diffraction pattern indicates a predominantly hcp structure of the Ru spacer. Patterns taken after deposition of a doped $Co_{92}Ag_8$ layer on top of the Ru spacer layer are shown in Figs. 1(g) and 1(h). A surprising feature is that the doped Co layer follows the hcp morphology of the Ru spacer layer. Therefore it appears that a few percent of Ag stabilize the hcp phase. This observation is corroborated by the x-ray measurements taken from test samples of pure and doped 80-Å-thick Co films, grown directly onto Ru buffer layers. The corresponding θ-2θ x-ray scans are shown in Fig. 2 for (a) a pure Co layer, (b) a Co layer with 5% Ag doping, and (c) one with 10% Ag doping. The inset shows the region around the fcc (222) and the hcp (0004) Bragg peaks, from

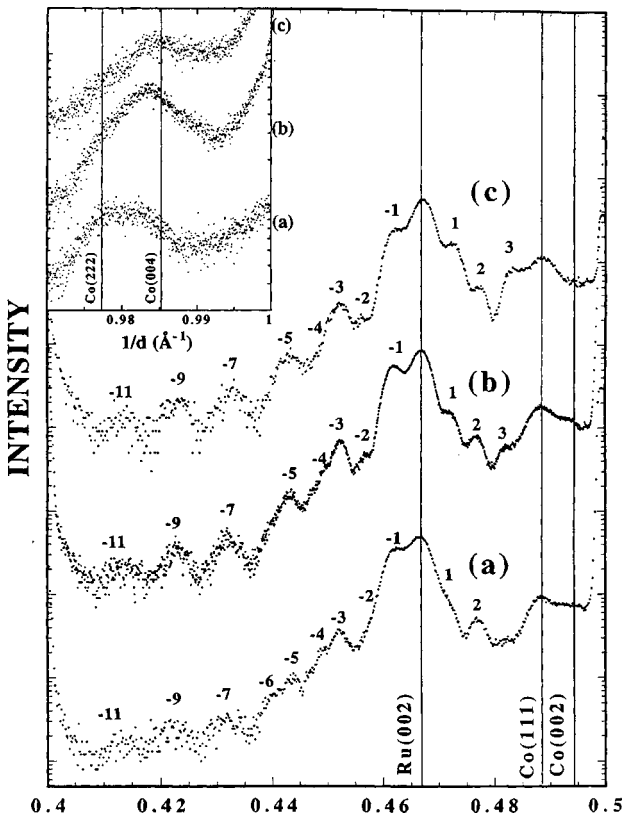

FIG. 2. θ-2θ x-ray scans for a pure Co layer (a), a Co layer with 5% Ag doping (b), and one with 10% Ag doping. The inset is the region around the fcc (222) and the hcp (0004) Bragg peaks. Also seen are the reflections for the Ru buffer and the large number of satellites of the Ru/Co/Ru structure that confirm the high crystalline quality of the films.

which it is evident that with increasing concentration of Ag impurities the Co reflections sharpen as they move to characteristic hcp positions. The main section of Fig. 2 shows the same feature, albeit somewhat less visible owing to the smaller angular separation, between the cobalt (111) and (0002) reflections. Also seen are the reflections for the Ru buffer and a large number of satellites of the Ru/Co/Ru structure that confirm the high crystal quality of the films.

Because Co and Ag are immiscible metals, the substrate temperature was held at 240 K to discourage clustering of the Ag within the top Co layer. Cross-sectional transmission-electron microscopy indicates that phase separation had been very effectively suppressed and that the size of any Ag clusters is less than the resolution of the instrument. This places an upper limit of 10 Å on the size of possible clusters.

The total thickness of the doped Co layer (32 Å) was kept the same as in the undoped Co layer. The top Co layer of each multilayer was capped with 30 Å of Ru to produce symmetric structures and prevent oxidation at the surface of the magnetic layer.

For the trilayer systems with Cu as the spacer layer material, 10 Å of Cu was deposited at the interfaces between the Ru buffer and the first Co layer as well as between the top Co layer and the Ru capping layer in order to maintain interface symmetry. Each Co layer in the Co/Cu/Co trilayer structures was 24-Å thick. The RHEED patterns observed along the [110] and [100] directions for the sequence indicate epitaxial pseudomorphic growth. As the Cu growth proceeds, the streaks become more intense and thinner with a marked decrease of spot intensity. This indicates that the Cu tends to adopt a two-dimensional growth mode that is almost certainly favored by the small lattice mismatch between Co and Cu. Moreover, RHEED images from the impure Co layer grown on top of the Cu display the same features. Furthermore, NMR experiments on similar samples have clearly indicated that the Co layers are stabilized in the hcp phase when deposited on Cu.[22]

III. EXPERIMENT

The bilinear interlayer exchange-coupling coefficient A_{12} (as defined in Ref. 23) as a function of the spacer-layer thickness as well as a function of the doping concentration was investigated using a superconducting quantum interference device (SQUID) and alternating gradient magnetometry (AGM) and ferromagnetic resonance (FMR). For small interlayer thicknesses, A_{12} was estimated from the saturation field values of the in-plane hysteresis loops using $H_{\rm sat} = 2A_{12}/tM_s$,[23] with $H_{\rm sat}$ the saturation field and M_s the saturation magnetization. For larger interlayer thicknesses the sign and strength of the interlayer coupling A_{12} was deduced from the FMR's as outlined in more detail below.

In accordance with predictions from quantum interference theories, long-period oscillations were observed for the two spacer materials with oscillation periods of about 12–20 Å. In addition, a large nonoscillatory component to the coupling was found for the systems with Ru as the spacer material. This nonoscillatory bias is independent of the doping concentration of the magnetic layer and may indicate a large superexchange component[21] to the coupling.

The AGM and SQUID hysteresis data show a linear dependence of the average magnetization on the applied field for antiparallel coupled structures, indicating a dominant bilinear antiferromagnetic interlayer coupling. Higher-order biquadratic interlayer coupling terms could not be detected within experimental uncertainties for any of the samples, which is also confirmed by the FMR results. From the SQUID and AGM measurements the saturation magnetization was deduced and used as an input parameter for the fits of the FMR modes.

FMR experiments have revealed two resonance modes with different intensities. These modes are known as acoustic and optic modes and correspond to the in-phase and out-of-phase precession of the magnetization in the separate ferromagnetic films.[24,23] A strong signal identifies the acoustic mode and a weak signal identifies the optic mode. An optic mode was observed for all samples, including the undoped Co/Ru/Co reference. This indicates that slight differences in growth for the first and second ferromagnetic Co layers result in small differences in the effective internal fields of the two layers, which allows the optic mode to have a small net dynamic magnetic moment. This small fluctuating net moment is then visible as a weak absorption peak in FMR experiments.

The FMR experiments were carried out as a function of the angle between the applied field and the layer plane. This angular dependence (ranging from 0° to 90°) of the acoustic and optic mode were fitted simultaneously to a model for

arbitrary magnetization configurations.[23] From this fit, the sign and strength of the interlayer coupling (A_{12}), the gyromagnetic ratio (g), and the effective anisotropy field (H_{eff}) were deduced with a maximum error of 10% for H_{eff} and A_{12}. Here H_{eff} is given in terms of the uniaxial anisotropy field H_a and the saturation magnetization M_s: $H_{\text{eff}}=4\pi M_s - H_a$. With M_s determined from SQUID measurements, H_a is deduced from H_{eff}. Typical parameters, e.g., common to all samples in the Co/Ru/$Co_{1-x}Ag_x$ trilayer series were $g = 2.15 \pm 0.1$ and an effective uniaxial anisotropy field H_{eff} that ranged between 5.5 and 8 kOe for samples of different doping concentration. H_{eff} did not appear to vary systematically with spacer thickness or dopant concentration and was reasonably constant for samples within a series of constant dopant concentration with variations of ± 0.6 kOe.

IV. PHASE SHIFTS FOR Co/Ru/$Co_{1-x}Ag_x$ AND Co/Cu/$Co_{1-x}Ag_x$

A. Co/Ru/$Co_{1-x}Ag_x$

First, the results for Co/Ru/$Co_{1-x}Ag_x$ trilayers are discussed with $x=0$, 0.03, 0.068, and 0.08. Here the Ru spacer layer varies in thickness between 9 and 30 Å and the Co and $Co_{1-x}Ag_x$ layers were held at 32 Å.

Typical examples of FMR absorption derivative spectra as a function of the applied field are shown in Fig. 3 for different Ag concentrations of $x=0$, 3, 6.8, and 8%. Measurements are shown for three different Ru thicknesses for each Ag concentration. The acoustic mode is associated with the largest signals. The 5×-amplified signal of the weak optic modes are inserted in Fig. 3 and the corresponding mode positions are indicated by arrows. When the coupling is parallel ($A_{12}<0$) the optic resonance lies on the low-field side of the acoustic mode, and when the coupling is antiparallel ($A_{12}>0$) the optic mode lies on the high-field side of the acoustic mode. The magnitude of the difference between the acoustic and optic resonance fields depends directly on the sign and strength of the interlayer coupling. From Fig. 3 it is seen that the position of the optic mode relative to the acoustic mode changes with increasing Ru thickness in a series with fixed Ag concentration and thus demonstrates the oscillatory coupling between the magnetic layers. More remarkably however is that such an oscillatory behavior can also be seen as a function of increasing doping concentration for *fixed* interlayer thickness. Comparing the position of the modes for the same thickness but increasing Ag doping concentration it is seen that the coupling oscillates between ferromagnetic coupling (F), zero coupling (ZC), and antiferromagnetic coupling (AF). This change of the sign of the coupling at fixed interlayer thickness therefore indicates that the phase ϕ of the oscillatory coupling A_{12} has shifted.

Figure 4(a) summarizes the thickness dependence of the interlayer coupling for all Co/Ru/$Co_{1-x}Ag_x$ trilayers with Ag concentrations of 0, 3, and 8%. The undoped Co film structure (0%) serves as a reference. Qualitatively there appears to be a single period for the oscillatory coupling that is independent of the Ag concentration, which means that the Ag does not affect the coupling period within experimental error. The position of the maxima however is clearly shifted by the Ag concentration, which is most obvious for the 3% doping, with a complete change in the sign for all Ru spacer-

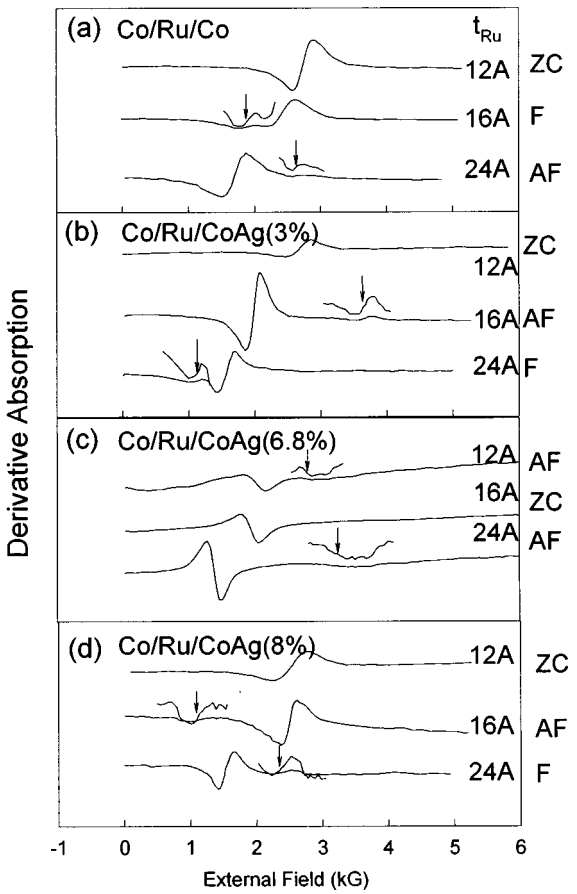

FIG. 3. In-plane FMR absorption derivative spectra as a function of the applied field for samples of different Ru thickness and Ag concentration. The structures are Co/Ru/$Co_{1-x}Ag_x$ wherein (a) $x=0$, (b) $x=0.03$, (c) $x=0.068$, and (d) $x=0.08$. The strongest peak is associated with the acoustic mode. The weaker peak is associated with the optic mode and is shown as an inset with a magnification of 5×. The optic-mode peak position is indicated by the arrows. ZC denotes zero coupling, F denotes ferromagnetic coupling, and AF denotes antiferromagnetic cooling.

layer thicknesses. This suggests that the phase ϕ of the oscillatory coupling is controlled by the Ag doping, increasing continuously up to a complete 360° phase shift at 8% Ag concentration.

The Ruderman-Kittel-Kasuya-Yosida theory of the oscillatory interlayer coupling suggests an analysis of the thickness dependence of the coupling strength using a functional form given by

$$J_0 = A \sin(2\pi t/L + \phi)/t^2. \tag{1}$$

Here the amplitude of the coupling is A, the period is L, and the thickness of the spacer layer is t. A phase factor ϕ is included to account for the observed phase shift as a function of the doping concentration. The functional form of Eq. (1), however, does not adequately describe the observed values for the coupling for thinner interlayer thicknesses shown in Fig. 4. Closer examination of the data reveals an apparent additive thickness-dependent bias J_b, decaying exponentially with increasing spacer thickness:

$$J_b = Be^{-t/d}. \tag{2}$$

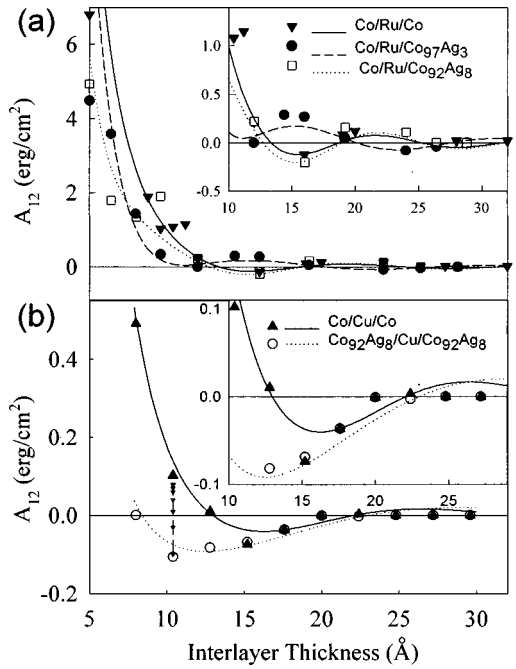

FIG. 4. (a) The experimentally determined (points) interlayer exchange coupling A_{12} in $Co/Ru/Co_{1-x}Ag_x$ trilayers vs the Ru spacer-layer thickness for $x=0\%$, 3%, and 8%. (b) The interlayer exchange coupling A_{12} in $Co_{1-x}Ag_x/Cu/Co_{1-x}Ag_x$ trilayers vs the Cu spacer-layer thickness for $x=0\%$ and 8%. Positive values correspond to antiparallel coupling and the solid and dotted lines are fits to the data using Eq. (3). The errors of the experimental data points lie within the size of a single point. The errors of the corresponding fits to Eq. (3) are given in the table caption of Table I. Further experiments on the phase shift using Cu, Au, and Ru as the doping material are shown in Fig. 8.

Here B is the amplitude of the bias and d is the decay length. The exchange coupling across the Ru has then the form

$$A_{12}=J_b+J_0. \tag{3}$$

Fits to the data using the five parameters in Eq. (3) are indicated in Fig. 4 by the full and dotted lines. The corresponding fit values for A, B, L, ϕ, and d are listed in Table I. Errors are given in the table caption. The magnitudes of the oscillatory and bias terms, as well as the period and decay length, are, within experimental error, independent of the Ag concentration. The phase, however, is clearly very sensitive to small changes in the Ag concentration and a concentration of as little as 8% is sufficient to change the phase by 360°. This continuous phase shift with increasing doping concentration suggests an oscillatory behavior of the phase for even higher doping levels.

While it may appear that a fit with five parameters is rather ambiguous, it is noted that the form of J_o is used to fit the data at larger interlayer thickness and the form of J_b is used to fit the data at smaller interlayer thicknesses. It is furthermore emphasized that it is not attempted here to yield a complete fit to the data. The purpose of the fit using Eq. (3) is to quantify the trend that small amounts of Ag added to the magnetic layer have a large effect on the coupling phase. This trend can be unambiguously seen in the data of Figs. 3 and 4 for the Ag concentrations of 0 and 3% revealing a nearly 180° shift.

Furthermore, the additive form of Eq. (3) needs some justification. The large value of A_{12} for small interlayer thicknesses might suggest an analysis of the data using a multiplicative rather than an additive functional form for the coupling, such as

$$A_{12}=J_b\cdot J_0. \tag{4}$$

Coupling of the form in Eq. (4) might be expected for a structure with rough interfaces or possibly due to proximity effects for small spacer thicknesses.[25] Equation (4) predicts that A_{12} oscillates between positive and negative with increasing phase shift at each interlayer thicknesses. This is in contrast to the data shown in Fig. 4(a), where for small interlayer thicknesses A_{12} is always positive, irrespective of the phase change.

B. $Co_{92}Ag_8/Cu/Co_{92}Ag_8$

Since the Ag appears only to affect the ferromagnetic side of the interfaces, one would expect a Ag concentration-dependent phase shift regardless of the nonmagnetic spacer material. With this in mind, a series of doped $Co_{92}Ag_8/Cu/Co_{92}Ag_8$ trilayers were prepared using Cu as the spacer material.

The interlayer coupling A_{12} as a function of the Cu spacer-layer thickness is shown in Fig. 4(b) for one trilayer structure with pure Co layers and another one with a doped Co layer, $Co_{92}Ag_8/Cu/Co_{92}Ag_8$. A clear shift of the first

TABLE I. Best-fit parameters of Eq. (3) to the $Co/Ru/Co_{1-x}Ag_x$ and $Co/Ru/Co_{1-x}M_x$ data ($M=$ Ag, Au, Ru, Cu). The parameters are the strength A, oscillation period L, and phase ϕ of the oscillatory coupling and the strength B and the decay length d of the bias term. A variation of the fit parameters of $\Delta A=\pm 10\times 10^{-16}$ ergs, $\Delta L=\pm 1$ Å, $\Delta B=\pm 40$ ergs/cm^2 and $\Delta d=\pm 0.1$ Å result in a similar fit with a variation of the phase on the order of $\Delta\phi=\pm 20°$.

Structure	A (10^{-16} ergs)	L (Å)	ϕ (deg)	B (ergs/cm^2)	d (Å)
Co/Ru/Co	35.8	12.8	192.5	240	1.7
$Co/Ru/Co_{97}Ag_3$	39.8	15.0	57.3	240	1.6
$Co/Ru/Co_{93}Ag_7$	47.0	12.8	−90	240	1.5
$Co/Ru/Co_{92}Ag_8$	49.7	12.8	−172	243	1.4
$Co/Ru/Co_{92}Cu_8$	98.1	12.8	−201	265	1.4
$Co/Ru/Co_{92}Au_8$	75.5	12.3	−212	210	1.5
$Co/Ru/Co_{92}Ru_8$	75.0	12.8	−150	250	1.2

TABLE II. Best-fit parameters of Eq. (3) for the $Co_{1-x}Ag_x/Cu/Co_{1-x}Ag_x$ system. The parameters are the strength A, oscillation period L, and phase ϕ of the oscillatory coupling and the strength B and the decay length d of the bias term. Errors correspond to those stated in Table I.

Structure	A (10^{-16} ergs)	L (Å)	ϕ (deg)	B (ergs/cm^2)	d (Å)
Co/Cu/Co	12	20.3	−33.2	28	1.8
$Co_{92}Ag_8/Cu/Co_{92}Ag_8$	18	29.9	83.1	20	1.2

maximum is apparent when Ag is added to the Co layers although the oscillations are long and less complete than those in the Ru systems.

A fit to the data was made using Eq. (3) and is shown by the solid line in Fig. 4(b). Values for the amplitudes, periods, decay lengths, and phases are tabulated in Table II. The addition of the Ag does not significantly change any parameter within the experimental uncertainties except for the phase. The repositioning of the first maximum with 8% Ag doping corresponds to a large phase shift of 120°. This shift, while not as large in magnitude as the shift observed for the Ru system, still indicates a specific effect on the coupling phase associated with the addition of Ag to the Co layers. It should be noted that the amplitude B of the bias term J_b from Eq. (2) was significantly smaller for the Cu system compared to the Ru system. Furthermore, for the systems with Cu spacer layers it was not possible to distinguish between an additive bias, as in Eq. (3), from a multiplicative bias in Eq. (4).

V. MECHANISM FOR THE PHASE SHIFT WITH INCREASING AG CONCENTRATION

The importance of the ferromagnetic layer for the phase of the oscillatory interlayer coupling is explained through a simple argument based on Bruno's quantum interference model.[11] The spin-dependent reflection coefficients at the interfaces are determined by the matching of the energy bands at the interface. A change of the complex reflection coefficients, due to changes of the band structure on either side of the interface, results directly in a change in the coupling phase.[11] This dependence is expressed alternatively by Mathon *et al.*,[26] who show that, using a single-band model, the phase of the coupling is strongly dependent on the potential step experienced by electrons traveling across the interface. In order to explain the observed phase shifts in the doped Co/Ru/CoAg and CoAg/Cu/CoAg trilayer structures, one therefore has to investigate the effect of the Ag on the electronic band structure in the Co layer.

Before addressing the electronic properties it should be emphasized that the SQUID and FMR data did not indicate any systematic Ag concentration-dependent changes in the saturation magnetization M_s, the coercive field H_c, or in the effective out-of-plane anisotropy field H_{eff}. Furthermore, as mentioned in Sec. II, RHEED patterns and x-ray data suggest that Ag doping stabilizes rather than modifies, the hcp growth of the Co layers. In particular, the small full width at half maximum ($<1°$) of the x-ray rocking curves indicate that the sample quality of the doped cobalt films is excellent. These considerations, together with the observed high epitaxial quality of the doped Co layers and the small diameter of the Ag clusters (less than 10Å, see Sec. II), suggest that the effects of the Ag dopants on the magnetic properties of the Co are small and that the Ag did not lead to a degradation of the structure or the magnetic properties of the Co layer. The introduction of Ag into the Co layer is hence interpreted to directly affect the phase of the bilinear interlayer exchange coupling and is not an artifact of structural or magnetic changes.

Interestingly, this effect is quite specific by only altering the phase of the coupling without modifying the coupling amplitude or oscillation period. This is consistent with the quantum interference models of the interlayer exchange coupling[10,11] in which the oscillation period is primarily determined by the stationary points on the spacer-layer Fermi surface. The insensitivity of the period of the coupling to the Ag doping concentration implies that the Ag dopants in the Co layer did not alter the Fermi level or topology of the Ru spacer layer. Furthermore, the fact that the coupling amplitude does not change indicates that the electron confinement in the spacer layer did not change significantly. Hence the amplitude of the reflection coefficients and thus the band structure of the ferromagnetic layer does not change significantly.

In order to investigate the effect of small concentrations of Ag on the electronic band structure of the Co layer, *ab initio* band-structure calculations were performed. Since the Ag-doped Co system is not a homogeneous solid solution, the actual electronic structure can only be approximated by studying model distributions of Ag atoms in a host Co lattice. The calculations presented here were performed for doped fcc Co on a Cu substrate. The doped Co was approximated by calculating large fcc unit cells with some face-centered Co atoms replaced by Ag atoms. The total number of unit cells was eight containing a total number of 32 atoms.

The electron-energy band-structure calculations were made using the tight-binding linear muffin-tin orbital atomic-sphere approximation[27] with spin-orbit interactions taken into account in the form proposed by Min and Jang.[28] A Perdew-Wang potential with nonlocal terms was used.[29] The standard combined corrections were included to compensate for errors due to the atomic-sphere approximation.[29] An experimental value of the lattice constant was taken (6.831 49 a.u. or 3.615 Å) equal to the lattice constant of a fcc Cu substrate.[30] The average value of the Wigner-Seitz radius was determined from experimentally measured lattice constants. Different values of the Wigner-Seitz radii for the Ag and Co atoms in inequivalent positions were used to minimize errors due to overlapping muffin-tin spheres.

From these calculations the total density of states (DOS) for ferromagnetic Co with a fraction of the Co atoms replaced by Ag were deduced. In general, magnetic moments of the Co atoms were found to be slightly different at various inequivalent positions, and a very small magnetic moment appeared at the Ag positions. Furthermore, the calculations

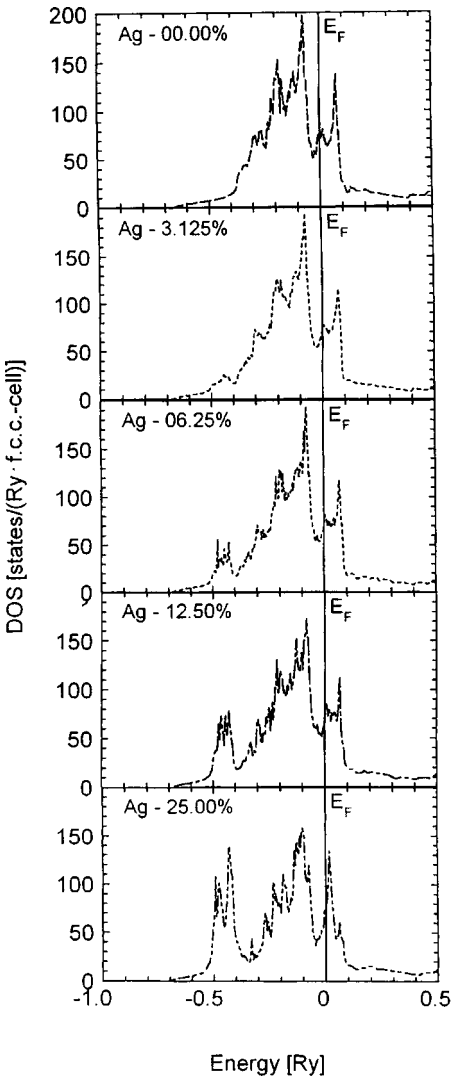

FIG. 5. Effect of Ag on the electronic DOS of Co. Cobalt atoms were replaced by Ag atoms in a fcc structure in order to imitate the effects of doping.

show that on the average 0.25 electrons per Ag atom are transferred from the Ag to the Co host (Fermi sea).

The total DOS is shown in Fig. 5 for various Ag concentrations ranging from 0 to 25%. At small concentrations, the Ag mainly adds states to the bottom of the band, far from the Fermi level. The changes at the bottom of the band are small on the scale of the DOS and cannot be resolved in Fig. 5. Therefore the shift of the bottom of the band due to the addition of Ag is summarized in Fig. 6, where the bottom band limit of the electron energy DOS relative to the bottom band limit of the undoped Co case is plotted as a function of the Ag concentration. The dashed line in Fig. 6 is a guide for the eye. At a Ag concentration of 8%, the shift in the potential is on the order of 0.4 eV. The two points at the concentration of 25% denote calculations performed for fcc Co (circles) and hcp Co (triangle). The difference in the shifts for hcp and fcc Co is small relative to the overall shift due to the doping.

The consequence of adding small amounts of Ag to the Co layer for the interlayer coupling can be stated as follows. Due to the Ag, electronic states with dominantly *s* character are added to the bottom of the band. This addition is equivalent to lowering the overall band limit of the doped Co layer. Via *sd* hybridization the itinerant conduction electrons will experience such a shift of the lower band limit as a shift in the effective potential. Hence the potential step at the interface is different for interfaces between the spacer layer and the pure Co layer and for interfaces between the spacer layer and the doped Co layer. Such a difference in the potential step should then, in accordance with the quantum interference model, result in different reflection coefficients and thus in different coupling phases.

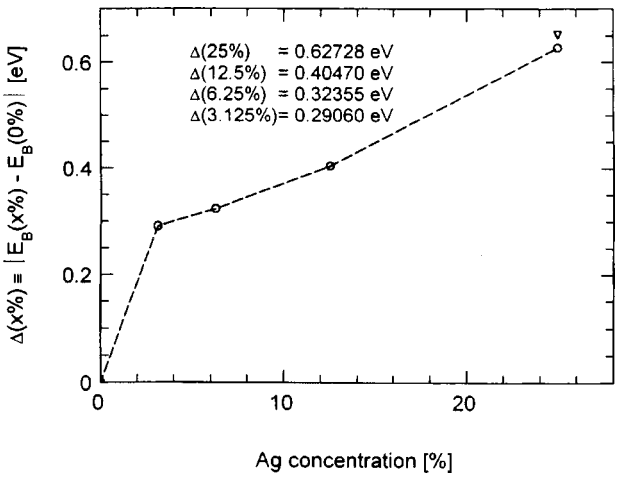

FIG. 6. The change in the position of the lower band limit with respect to the undoped Co band limit as a function of the Ag concentration. Two data points for 25% were calculated corresponding to an fcc (circle) and an hcp (triangle) Co layer, whereas all other points are for an fcc Co layer.

In order to assess whether a potential shift on the order of 0.4 eV (as deduced from Fig. 6 for 8% Ag doping) is sufficient to produce a significant phase shift in the oscillatory exchange coupling, the interlayer coupling is calculated as a function of the position of the lower band limit. A calculation of the coupling using *ab initio* techniques such as those in Fig. 5 is quite demanding numerically because of the small differences in energy involved and the large number of atoms needed to properly describe the low Ag concentrations. A different approach, using a two-band tight-binding model,[31] was instead taken with the intent to demonstrate qualitatively that small potential shifts can indeed produce large phase shifts in the interlayer coupling.

In this approach the trilayer is represented through a finite number of atomic layers. Ten atomic layers represent each ferromagnetic layer, and the magnetic layers are separated by 2 to 20 nonmagnetic atomic layers representing an intervening Cu spacer. Two sets of orbitals in an hcp lattice, periodic in the plane of the atomic layers, are included with energies that depend on (material specific) potentials $E_{\alpha\sigma}$. The subscripts are defined as follows: α indicates the band and σ the spin state. Hopping integrals $\gamma_{\alpha\sigma}$ are defined, associated with each of the two orbitals.

The resulting set of coupled equations are solved for electron energies ε. The electron energies for both spin states are summed over the entire Brillouin zone and compared for parallel-aligned and antiparallel-aligned ferromagnetic layers. The exchange-coupling energy is calculated as the difference between these two total energies:

TABLE III. Tight-binding parameters for the two-band model described in the text. Shown are the spin-dependent potentials E_+ and E_-, and hopping integrals γ for each band in each material. All values are in eV.

		s band			*d* band		
Material	γ_{sd}	γ_{ss}	E_+	E_-	γ_{dd}	E_+	E_-
Co	0.45	1.38	−0.47	−0.77	0.33	−0.49	−1.26
Cu	0.35	1.34	−0.99	−0.99	0.21	−2.24	−2.24

$$J=\left\{\sum_{\varepsilon<\varepsilon_f}(\varepsilon-\varepsilon_f)\right\}_{\text{parallel}}-\left\{\sum_{\varepsilon<\varepsilon_f}(\varepsilon-\varepsilon_f)\right\}_{\text{antiparallel}}. \quad (5)$$

The Fermi energy ε_f is set at zero. Parameters are chosen to roughly represent essentials of the Co and Cu layers. They are summarized in Table III.[32] Note that the coupling strength and phase is sensitive to the magnitudes of the overlap integrals γ_{ss}, γ_{dd}, and γ_{sd} at the interfaces. These are calculated as geometrical averages of the corresponding bulk values from each side of the interface.[25] Which particular overlap integral has the largest effect depends on the crystal structure.

The potentials of the *s* bands in the magnetic layers were varied by an amount Δ, representing a small change in the average *s*-band potential due to Ag impurities. The point of this calculation is to show how Δ affects the phase, and for simplicity the position of all bands relative to $\varepsilon_f=0$ is assumed independent of the number of layers.

Results of the calculation outlined above are presented in Fig. 7 where *J*, defined in Eq. (5), is shown as a function of the number of interlayers N_s for different values of Δ. A long-period oscillation is evident and consistent with the choice of parameters for the overlap integrals and potentials. The effects of small changes in the *s*-band potential of one of the ferromagnetic layers is quite dramatic. A change in the phase of the coupling of approximately 150° occurs for $\Delta=0.4$ eV. Note that Δ has no effect on the period or amplitude of the coupling. Also, the sensitivity of the phase to the small Δ values is heightened by the small splitting of the *s* bands in the Co. Without this splitting, the dependence of the phase on Δ is much weaker.

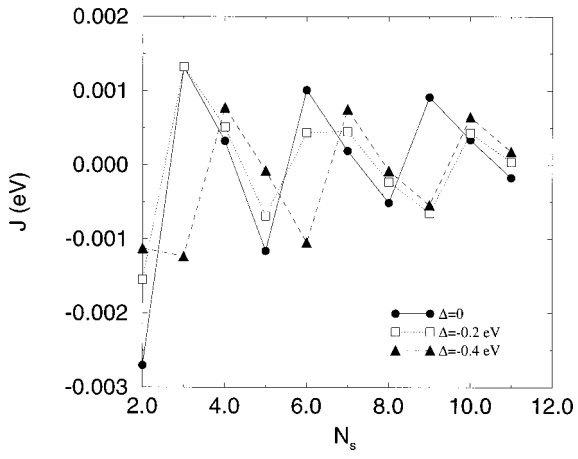

FIG. 7. Results of the calculations for interlayer exchange calculations for *J* based on Eq. (5) using the two-band model described in the text. The exchange coupling is shown as a function of Cu thickness for shifts △ in the *s*-band potential of the ferromagnetic layers. Note the nearly 150° change in the phase of the coupling with a △ of only 0.4 eV.

The preceding considerations support the conjecture that small amounts of Ag contribute electronic energy states to the lowest portion of the Co bands, effectively shifting the *s* band without other substantial changes to the overall DOS for small doping concentrations. This shift of the conduction band changes the magnitude of the potential step at the interface between the ferromagnet and the spacer layer. As calculated from the two-band model above, this change in the step height, although small, is large enough to account for large phase shifts in the interlayer coupling on the order of 150°.

The mechanism described above for Ag-induced phase shifts is in qualitative agreement with the measurements made on the $Co/Ru/Co_{1-x}Ag_x$ and $Co_{92}Ag_8/Cu/Co_{92}Ag_8$ systems. In the next section, results from experiments on trilayer structures using different dopants are presented that are also consistent with this interpretation.

VI. PHASE SHIFTS, BIASING, AND DOPANTS IN OTHER SYSTEMS

Several additional systems were studied in order to test the phase-shift mechanism proposed in Sec. V and to investigate the additional bias observed in the Co/Ru and Co/Cu structures. Two systems were studied: (1) $Co/Ru/Co_{92}M_8$ where $M=$ Au, Ru, Cu and (2) $Co_{92}Ag_8/Co/Cu/Co/Co_{92}Ag_8$. Results and interpretation of the measurements are presented below.

A. $Co/Ru/Co_{92}M_8$

As evidenced by the data shown in Fig. 4, doping with Ag affects the phase of the coupling in both Co/Ru and Co/Cu structures consistent with the arguments of the previous section. If the doping is indeed changing the effective potential at the Co/Cu and Co/Ru interfaces, then other dopants should display similar effects. In particular, Cu and Au, having the same valence structure as Ag, should produce similar changes in the effective potential and thus similar phase shifts.

This hypothesis was investigated using $Co/Ru/Co_{1-x}M_x$ structures where $M=$ Au, Cu, and Ru. The results are summarized in Fig. 8(a) and the fit parameters to Eq. (3) are listed in Table I. The phase shifts for 8% Au and 8% Cu dopants are both near −200°, within 15% of the −172° shift observed for 8% Ag. Note also that the amplitude and period are relatively *unaffected* by doping. The effects of doping

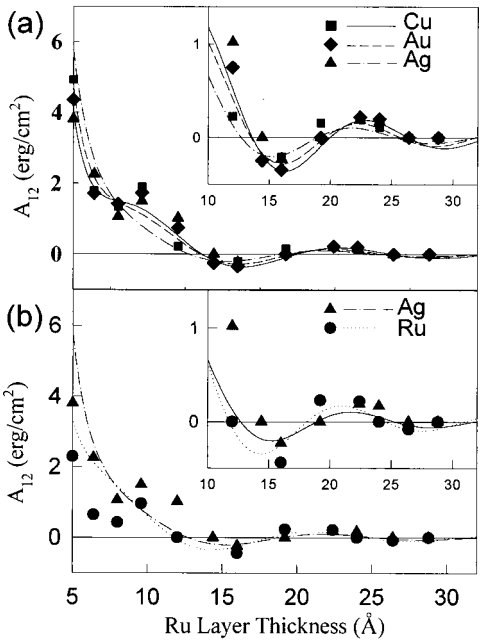

FIG. 8. (a) The interlayer exchange coupling A_{12} in Co/Ru/$Co_{92}M_8$ trilayers vs the Ru space-layer thickness for M = Cu, Au, and Ag. (b) The interlayer exchange coupling A_{12} in Co/Ru/$Co_{92}M_8$ trilayers vs the Ru spacer-layer thickness for M = Ag and Ru. The solid lines are fits to the data using Eq. (3).

with Ru, an element from a column left of Co in the Periodic Table, were examined for a Co/Ru/$Co_{92}Ru_8$ series. The observed phase shift with $-150°$ is smaller than the one for Cu and Au, but is in line with the one for the Ag doping.

B. Interface effects in $Co_{92}Ag_8$/Co/Cu/Co/$Co_{92}Ag_8$

If the phase shifts were due to structural modifications localized only to the interface region, then it would be expected that the phase shifts should completely disappear with the addition of only one or two pure Co layers between the Cu spacer layer and the doped Co layers. Therefore, the following experiment was performed in order to test whether the effects of doping on the phase of the exchange coupling were linked to modifications of the interface structure. A series of samples was grown where pure interfacial Co layers were inserted between the Cu spacer and the doped $Co_{92}Ag_8$ layers. The total thickness of the Co/$Co_{92}Ag_8$ layer was kept at 24 Å and the Cu spacer was kept at 10 Å.

It is found that with increasing interfacial Co layer thickness the coupling strength changes continuously from a value corresponding to a doped $Co_{92}Ag_8$/Cu/$Co_{92}Ag_8$ trilayer (i.e., no interfacial Co layer) towards a value corresponding to an undoped Co/Cu/Co trilayer. The results are shown in Fig. 4(b) by the points at the interlayer thickness of $t = 10$ Å, where the bottom point coincides with the $Co_{92}Ag_8$/Cu/$Co_{92}Ag_8$ trilayer and the top one corresponds to a trilayer $Co_{92}Ag_8$/Co/Cu/Co/$Co_{92}Ag_8$ with 7 ML of interfacial Co. This increase of the exchange coupling as a function of the interfacial Co layer thickness d is shown separately in Fig. 9.

From the results in Figs. 4(b) and 9 it is concluded that the coupling phase changes continuously upon insertion of a few pure Co layers, which is consistent with the idea that the interfacial Co layer introduces an additional step in the electronic potential. This additional potential step modifies the total phase shift of the oscillatory coupling. With increasing thickness of the interfacial Co layer, the phase shift is therefore expected to change from that of the doped material to that of the pure Co. Interestingly, this change of A_{12} as a function of the interfacial Co layer thickness d can be fit to an exponential of the form

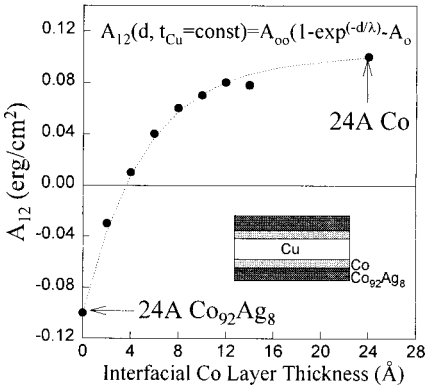

FIG. 9. The interlayer coupling strength A_{12} in $Co_{92}Ag_8$/Co/Cu/Co/$Co_{92}Ag_2$ as a function of the interfacial Co layer thickness. The total $Co_{92}Ag_8$/Co layer thickness was kept constant at 24 Å. The dotted line is a fit to Eq. (6).

$$A_{12}(d, t_{Cu}=\text{const}) = A_\infty(1-e^{-d/\lambda}) + A_0, \qquad (6)$$

with A_0 corresponding to the coupling strength for $d=0$ (no interfacial Co layer) and A_∞ corresponding to the coupling strength for pure Co layers without doping. The characteristic length λ is fitted to the data and has a value of approximately 5 Å.

Structural analysis of these samples also indicates that there is no measurable migration of Ag into the interface region. This and the results shown in Fig. 9 confirm that the effects of doping are not localized at the interface. The meaning of the exponential ''relaxation'' as a function of the interfacial Co layer thickness is not clear, but may be related to the dependence of the coupling phase on the magnetic layer thicknesses.[18]

VII. SUPEREXCHANGE BIAS

Fits using phenomenological forms for the interlayer coupling in the Co/Ru multilayers revealed an additive bias to the interlayer coupling in the structures with Ru as the spacer layer. This additive bias decreases exponentially with increasing Ru layer thickness. The decay length and strength of the bias are independent of doping concentration in the magnetic layer. A smaller bias was found for the Cu spacer-layer structures and furthermore could not be distinguished from a multiplicative contribution that might be identified with interfacial roughness.

The strong bias observed in the Ru spacer-layer samples is suggestive of a short-range additive superexchange coupling predicted by Shi, Levy, and Fry.[21] The existence of this component to the coupling requires the spacer material to have a large density of states just above the Fermi level. The existence of an observable antiparallel bias in the Ru but not

in the Cu is consistent with this conjecture because Ru possesses a large density of states near the Fermi level whereas Cu, with a nearly spherical Fermi surface, does not.

VIII. SUMMARY AND CONCLUSIONS

The effect of adding small amounts of nonmagnetic Ag, Au, Cu, or Ru to the ferromagnetic layer in Co/Ru/Co and Co/Cu/Co trilayers was examined. Large changes in the coupling phase of the oscillatory interlayer exchange coupling were observed with no significant changes to the coupling amplitude or period. These phase shifts could be traced through 360° with the addition of up to 8% Ag to one of the Co layers in trilayer structures with Ru as the spacer layer. A phase shift of 120° was observed when both cobalt layers were doped with 8% Ag in a trilayer with Cu as the spacer layer. Quantum interference models[11,13] predict a phase change in the oscillatory interlayer coupling when the complex reflection coefficients at the interface change due to changes in the band mismatch at interfaces or equivalently due to changes in the potential step that the electrons experience upon crossing the interface.[26] *Ab initio* band-structure calculations show that the addition of Ag to the Co host leaves the overall structure of the DOS unaltered and only changes the lower-lying electron states. This is interpreted as a change of the potential step at the interface.

The situation presented here differs from the one described in Refs. 17–19. There, the Fermi level was shifted considerably by increasing/decreasing the average number of electrons upon going from a pure Co layer, via a CoNi or FeNi alloy to a pure Ni or Fe layer, respectively. This change is explained through a gap in the Co band structure. Changing the number of electrons varies the position of the Fermi level with respect to this gap and thus changes the reflection phase as well as amplitude. In contrast, for the situation presented here, the insensitivity of the coupling amplitude upon doping indicates that the electronic properties around the Fermi level of the magnetic layer were not significantly altered. This is supported by the *ab initio* band-structure calculations for small amounts of Ag inserted into a Co host. The only significant effect visible in the calculated DOS plots of Fig. 5 are additional states at the *bottom* of the band that effectively correspond to a shift of the center of gravity of the Co *s* band to lower values. Such a shift can alternatively be justified through a charge-transfer concept from the Ag to the Co host. Ag has two electrons more than Co and can transfer electrons to the Co *s* band. This interpretation is supported by the band-structure calculations that give an average charge transfer of 0.25 electrons per Ag atom to the surrounding Fermi sea. For a fixed Fermi level, the bottom of the Co *s* band is then shifted with respect to the Fermi level. Via *sd* hybridization the itinerant electrons that are responsible for the interlayer exchange coupling will sense this shift in the effective potential. The details on how the band structure at the Fermi level is modified through the addition of nonmagnetic Ag, Cu, Au, and Ru cannot be inferred from the DOS plots presented. This requires much more detailed calculations of the band structure. Such calculations should then predict the relative size of the phase shift for the different doping materials such as Ag, Cu, Au, and Ru.

Using the charge-transfer concept, however, it is instructive to consider the phase shift versus the number of valence electrons, which is shown in Fig. 10. The phase of $Co/Ru/Co_{1-x}M_x$ with $M=$Ru, Ag, Cu, Co decreases with an increasing average number of valence electrons (increasing doping concentration). This is similar to the calculated decrease in phase with the increase in the number of electrons as given in Ref. 19. The phase shift observed here for $Co/Ru/Co_{1-x}M_x$, however, is much larger for the same number of electrons than the one in Ref. 19.

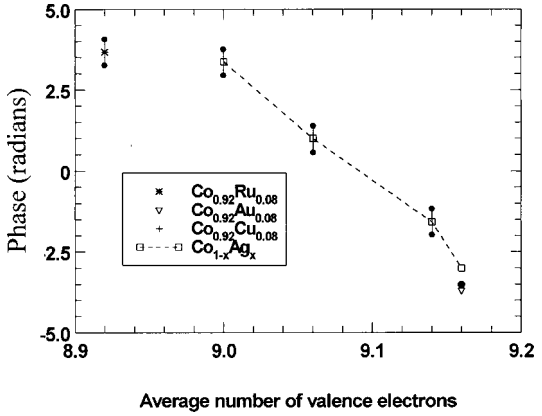

FIG. 10. The phase shift vs the average number of valence electrons in Co for $Co/Ru/Co_{1-x}M_x$ with $M=$Ag, Cu, Co, Ru. The average number of nine electrons corresponds to pure Co. The error bars correspond to the uncertainties in fitting the phase (see Table I).

It is emphasized that the observed phase shift is not believed to be due to any structural changes. The RHEED and x-ray data show that for the Co/Ru/CoAg system, the epitaxy of the cobalt is maintained in the presence of the silver impurities. This in turn suggests that the Co band structure may not be seriously modified, particularly at these low impurity concentrations. Furthermore, it might be argued that the overall hcp structure has improved upon doping given the reduced stacking fault density and better defined growth morphology. In addition, as shown in Fig. 6, the difference in the potential shifts between the fcc and hcp structure is significantly smaller than the shift due to doping. The stabilization of the hcp Co structure through doping is therefore not held responsible for the observed phase shift.

Furthermore, the observed effect is not an interface effect. Experiments wherein pure Co layers were added between the Cu spacer layer and the doped Co layer demonstrated that the phase shifts were not due to interface effects. The phase shift is continuously reduced, but not eliminated, even with the addition of seven pure Co layers between the Cu interface and the doped Co layer.

Finally it is noted that a large additive bias was observed for the trilayer structures with Ru as the spacer-layer material. Such a bias is consistent with a superexchange bias, predicted by Shi, Levy, and Fry,[21] resulting from a large DOS above the Fermi level. This is consistent with the observation for the Ru spacer layer that shows an additive bias and has large DOS at the Fermi level whereas for Cu the additive bias is less pronounced in accordance with a lower DOS above the Fermi level.

ACKNOWLEDGMENTS

This work was supported by the Brite-Euram HotSEAMS Programme No. BE96-3407, by NATO No. RG 930480, and by NSF-CNRS-9603252. L.Z., U.E., and P.W. were supported in part under NSF DMR-9400263 and the R. J. Yeh Fund. R.L.S. wishes to acknowledge support under NSF DMR-9703783. J.M. and A.S. wish to acknowledge the support from KBN Poland, under Grant No. 2 P302 005 07.

*Present address: Dept. of Physics, University of Western Australia, Nedlands, WA 6907, Australia.

[1] S. S. P. Parkin, Phys. Rev. Lett. **67**, 3598 (1991).

[2] S. T. Purcell, W. Folkerts, M. T. Johnson, N. W. E. McGee, K. Jager, J. aan de Stegge, W. B. Zeper, W. Hoving, and P. Grunberg, Phys. Rev. Lett. **67**, 903 (1991).

[3] M. T. Johnson, S. T. Purcell, N. W. E. McGee, R. Coehoorn, J. aan de Stegge, and W. Hoving, Phys. Rev. Lett. **68**, 2688 (1992).

[4] P. J. H. Bloemen, R. van Dalen, W. J. M. de Jonge, M. T. Johnson, and J. aan de Stegge, J. Appl. Phys. **73**, 5972 (1993).

[5] D. M. Edwards, J. Mathon, R. B. Muniz, and M. S. Phan, J. Phys.: Condens. Matter **3**, 4941 (1991).

[6] P. Bruno and C. Chappert, Phys. Rev. Lett. **67**, 1602 (1991).

[7] Z.-P. Shi, P. M. Levy, and J. L. Fry, Phys. Rev. Lett. **69**, 3678 (1992).

[8] M. van Schilfgaarde and F. Herman, Phys. Rev. Lett. **71**, 1923 (1993).

[9] P. Lang, L. Nordstršm, R. Zeller, and P. H. Dederichs, Phys. Rev. Lett. **71**, 1927 (1993).

[10] M. D. Stiles, Phys. Rev. B **48**, 7238 (1993).

[11] P. Bruno, J. Magn. Magn. Mater. **121**, 248 (1993); Phys. Rev. B **52**, 411 (1995).

[12] Since the coupling strength oscillates in a sinusoidal fashion as a function of the interlayer thickness, there is also a specific phase ϕ associated with this oscillatory behavior. This can be described in a phenomenological way through a functional form such as Eq. (1). A shift in the phase corresponds then to a shift of the maxima, minima, and zeros of the coupling strength to larger or smaller interlayer thicknesses.

[13] J. Barnas, J. Magn. Magn. Mater. **111**, L215 (1992); **128**, 171 (1994).

[14] P. J. H. Bloemen, M. T. Johnson, M. T. H. van de Vorst, R. Coehoorn, J. J. de Vries, R. Jungblut, J. aan de Stegge, A. Reinders, and W. J. M. de Jonge, Phys. Rev. Lett. **72**, 764 (1994).

[15] S. N. Okuno and K. Inomata, Phys. Rev. Lett. **72**, 1553 (1994).

[16] J. J. de Vries, A. A. P. Schudelaro, R. Jungblut, P. J. H. Bloemen, A. Reinders, J. Kohlhepp, R. Coehoorn, and W. J. M. de Jonge, Phys. Rev. Lett. **75**, 4306 (1995).

[17] M. T. Johnson, M. T. H. van de Vorst, P. J. H. Bloemen, R. Coehoorn, A. Reinders, J. aan de Stegge, and R. Jungblut, Phys. Rev. Lett. **75**, 4686 (1995).

[18] P. J. H. Bloemen, M. T. Johnson, M. T. H. van de Vorst, R. Coehoorn, A. Reinders, J. aan de Stegge, R. Jungblut, and W. J. M. de Jonge, J. Magn. Magn. Mater. **148**, 193 (1995).

[19] J. Kudrnovský, V. Drchal, R. Coehoorn, M. Šob, and P. Weinberger, Phys. Rev. Lett. **78**, 358 (1997).

[20] L. Zhou, Z. Zhang, P. E. Wigen, and K. Ounadjela, J. Appl. Phys. **76**, 7078 (1994); L. Zhou, Z. Zhang, P. E. Wigen, R. L. Stamps, K. Ounadjela, M. Hehn, and J. Gregg, IEEE Trans. Magn. **31**, 3924 (1995); K. Ounadjela, L. Zhou, R. Stamps, M. Hehn, Z. Zhang, P. E. Wigen, and J. Gregg, J. Appl. Phys. **79**, 4528 (1996).

[21] Z.-P. Shi, P. M. Levy, and J. L. Fry, Phys. Rev. B **49**, 15 159 (1994).

[22] N. Persat, A. Dinia, J. P. Jay, C. Meny, and P. Panissod, J. Magn. Magn. Mater. **156**, 371 (1996); **164**, 37 (1996).

[23] Z. Zhang, L. Zhou, P. E. Wigen, and K. Ounadjela, Phys. Rev. B **50**, 6094 (1994). Note: The definition of A_{12} in this paper corresponds to J of Ref. 1.

[24] B. Heinrich, Z. Celinski, J. F. Cochran, A. S. Arrott, K. Myrtle, and S. T. Purcell, Phys. Rev. B **47**, 5077 (1993).

[25] D. Stoeffler and F. Gautier, Phys. Rev. B **44**, 10 389 (1991).

[26] J. Mathon, M. Villeret, D. M. Edwards, and R. B. Muniz, J. Magn. Magn. Mater. **121**, 242 (1993).

[27] The TB-LMTO-ASA computer program (source code version 4.7) was made available by G. Krier, O. Jepsen, A. Burkhardt, and O. K. Andersen and the essentials can be found in O. K. Anderson, O. Jepsen, and M. Sob, in *Electronic Structure and its Application*, 2nd ed., edited by M. S. Youssouff (Springer, Berlin 1987).

[28] B. I. Ming and Y.-R. Jang, J. Phys.: Condens. Matter **3**, 5131 (1991).

[29] J. P. Perdew, J. A. Chevary, S. H. Vosko, K. A. Jackson, M. R. Pedersen, D. J. Singh, and C. Fiolhais, Phys. Rev. B **46**, 6671 (1992).

[30] J. J. de Miguel, A. Cebolada, J. M. Gallego, A. Miranda, C. M. Schneider, P. Schuster, and J. Kirschner, J. Magn. Magn. Mater. **93**, 1 (1991).

[31] B. R. Cooper and A. J. Bennett, Phys. Rev. B **1**, 4654 (1970).

[32] W. A. Harrison, in *Electronic Structure and the Properties of Solids* (Freeman, San Francisco, 1980).